Available online at www.sciencedirect.com
SCIENCE DIRECT
Polymer 46 (2005) 10574–10584
polymer
www.elsevier.com/locate/polymer

Poly(hydroxyether terephthalate ester): Synthesis, characterization and competitive specific interactions in mixtures with poly(ethylene oxide)

Bingquan Liu, Weian Zhang, Sixun Zheng*

Department of Polymer Science and Engineering, Shanghai Jiao Tong University, Shanghai 200240, People's Republic of China

Received 2 April 2005; received in revised form 19 July 2005; accepted 29 July 2005
Available online 15 August 2005

Abstract

A novel poly(hydroxyether ester) (PHEE), poly(hydroxyether terephthalate ester) (PHETE) was synthesized via the polymerization of diglycidyl ether of bisphenol A (DGEBA) with terephthalic acid catalyzed by tetrabutylammonium bromide (TBAB). From the structural view of point, PHETE combines the structural features of both poly(hydroxyether of bisphenol A) (PH) and poly(trimethylene terephthalate) (PTT). The miscibility and intermolecular specific interactions in the blends of PHETE and poly(ethylene oxide) (PEO) were investigated by means of differential scanning calorimetry (DSC) and Fourier transform infrared spectroscopy (FTIR). The PHETE/PEO blends displayed single, composition-dependent glass transition temperatures (T_gs), indicating that the blends are miscible in amorphous state, which was further confirmed by the depression of equilibrium melting point depression. FTIR studies indicate that there are the competitive specific interactions upon adding PEO to the system, which were involved with the intramolecular and intermolecular hydrogen bonding interactions, i.e. –OH···O=C<, –OH···–OH and –OH versus ether oxygen atoms of PEO between PHETE and PEO.
© 2005 Elsevier Ltd. All rights reserved.

Keywords: Poly(hydroxyether terephthalate ester); Poly(ethylene oxide); Miscibility

1. Introduction

Poly(hydroxyether ester)s (PHEE) are a class of novel thermoplastics derived from the reaction from diglycidyl ethers with diacids [1,2]. These polymers are of industry interest since they can combine good mechanical properties with processability and barrier properties [3]. More importantly, this class of materials displayed the typical biodegradability [4,5], which makes the materials a class of interesting candidates for environmentally benign materials. Due to the potential application, the investigations on the structure and properties of the polymers have begun to appear [6–11]. Most of the previous studies are concerned with the composite systems comprised of PHEE with some cereal products such as starch, protein [6–11]. Nonetheless, there are only very limited reports on miscibility and phase behavior of PHETE with biodegradable (or biocompatible) synthetic polymers. Willett et al. investigated the miscibility and intermolecular hydrogen bonding interactions of the blends of PHEE with poly(lactic acid) (PLA) [12–15]. In addition, all the previous reports were concerned with the PHEE prepared via diglycidyl ether of bisphenol A with aliphatic diacids whereas aromatic diacids (e.g. terephthalate acid) has scarcely been used.

In this work, we present synthesis of a novel poly(hydroxyether ester), poly(hydroxyether terephthalate ester) (PHETE). Terephthalate diacid is used to react with diglycidyl ether of bisphenol A (DGEBA), instead of aliphatic diacids used in the previous reports [6–15]. To the best of our knowledge, there are no precedent reports on PHETE. From the structural view of point, PHETE combines the structural features of both poly(hydroxyether of bisphenol A) (PH) and poly(trimethylene terephthalate) (PTT) (Scheme 1). The presence of both secondary hydroxyl and carbonyl groups endows the characteristics of the polymers with self-association. Upon adding PEO to PHETE, the competitive specific interactions could occur among –OH···O=C<, –OH···–OH and –OH versus ether

* Corresponding author. Tel.: +86 21 54743278; fax: +86 21 54741297.
E-mail address: szheng@sjtu.edu.cn (S. Zheng).

0032-3861/$ - see front matter © 2005 Elsevier Ltd. All rights reserved.
doi:10.1016/j.polymer.2005.07.095

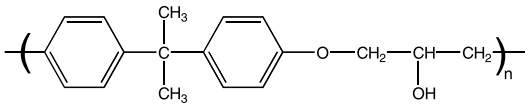

Poly(hydroxyether of bisphenol A) (PH)

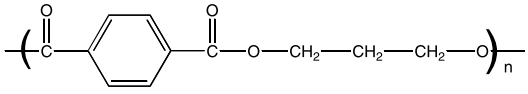

Poly(trimethylene terephthalate) (PTT)

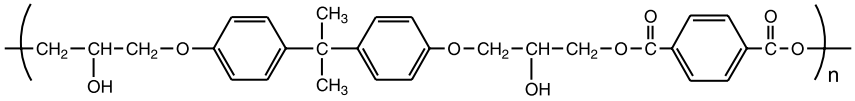

Poly(hydroxyether terephthalate ester) (PHETE)

Scheme 1. Structures of PH, PTT and PHETE.

oxygen atoms of PEO, (i.e. intra-chain versus inter-chain interactions). The PHETE/PEO blends could provide an ideal model system that allow investigating the competitive hydrogen bonding interaction in the binary blends of PHETE and PEO instead of in ternary systems comprise of PH, PTT and PEO. In the work, the miscibility of this blend system will be established based on differential scanning calorimetry (DSC) and the competitive hydrogen bonding interactions in the blends of PHETE with PEO will be addressed by means of Fourier transform infrared spectroscopy (FTIR).

2. Experimental

2.1. Materials

Diglycidyl ether of bisphenol A (DGEBA) was obtained from Shanghai Resin Co., China and it has an epoxide equivalence of 0.51. Before use, its molecular weight was measured to be $M_n = 385$ by means of vapor phase osmometry (VPO). Terephthalate acid and ethyl benzoate were of analytically pure grade, purchased from Shanghai Reagent Co., China. Poly(ethylene oxide) (PEO) was supplied by Shanghai Reagent Co., China and it has a quoted molecular weight of $M_n = 20{,}000$. Poly(hydroxyether of bisphenol A) (PH) was synthesized in this lab and it has molecular weight of $M_n = 28{,}000$, measured by gel permeation chromatography (GPC). All the solvents such as *N*,*N*′-dimethylformamide (DMF), tetrahydrofuran (THF) were obtained from commercial resources. Prior to use, toluene was purified by refluxing over calcium hydride (CaH_2) for 6 h and distilling under reduced pressure.

2.1.1. Synthesis of poly(hydroxyether terephthalate ester) (PHETE)

PHETE was synthesized by referencing the literature methods [1,2]. In a typical experiment, DGEBA (8.00 g, 0.20 mol) and terephthalate diacid (3.32 g, 0.20 mol) were charged into a three-necked flask equipped with a condenser and a mechanical stirrer. The reactants were dissolved in 15 ml *N*,*N*′-dimethylformamide (DMF) and 0.2 g of tetrabutylammonium bromide (TBAB) was added and used as a catalyst. The reactive system was refluxed with vigorously stirring for 24 h. The polymer product was precipitated in deionized water and dried in vacuo at 60 °C for 72 h. The polymer was subjected to the measurement of gel permeation chromatography (GPC) to obtain the molecular weights of $M_n = 12{,}000$ and $M_w = 19{,}000$.

2.1.2. Synthesis of 1,3-diphenoxy-2-propanol (DPP)

DPP was synthesized via the stoichiometric reaction of phenol and epichlorohydrin. In a typical experiment, 45 ml of 30% aqueous NaOH (13.6703 g, 0.34 mol) was dropped to phenol (32.1252 g, 0.34 mol) and the mixture was stirred for 20 min at 50 °C. Epichlorohydrin (10.5400 g, 0.10 mol) was slowly added to the system within 20 min and the system was refluxed for 3 h. The mixture was washed with chloroform three times and the organic phase was washed successively with 10 wt% aqueous NaOH and water and dried over anhydrous Na_2SO_4. The solvent was evaporated and the product was characterized by FTIR and NMR spectroscopy.

2.1.3. Preparation of polymer blends

The PHETE/PEO blends were prepared by solution casting from tetrahydrofuran (THF) at room temperature. The total polymer concentration was controlled within 5% (w/v). To remove the residual solvent, all the

blend films obtained were further desiccated in vacuo at 60 °C for 1 week.

2.2. Characterizations and measurement

2.2.1. Fourier transform infrared spectroscopy (FTIR)

The FTIR measurements were conducted on a Bruker Equnox 55 Fourier transform spectrometer at room temperature (27 °C). To obtain the FTIR spectra, the thin films of plain PHETE and its blends with PEO were cast onto KBr windows from 2 wt% DMF solution at 60 °C. The films obtained were further dried in vacuo at 60 °C for 2 weeks to remove residual solvent. All of casting films used in the study were sufficiently thin to be within a range where the Beer–Lambert law is obeyed. The FTIR spectra were recorded with 64 scans at a resolution of 2 cm^{-1} for signal accumulation. For the samples in the solution, a sealed cell with KBr windows and 0.2 mm sample thickness were used. Toluene was used as the solvent since it does not form polar interaction with the model compounds selected in this study. The model compounds of PHETE used in this work are ethyl benzoate (EB) and 1,3-diphenoxy-2-propanol (DPP) (Scheme 2), which stand for carbonyl moiety and the hydroxyl ether structural unit of PHETE, respectively.

2.2.2. Nuclear magnetic resonance spectroscopy (NMR)

The NMR measurement was carried out on a Varian Mercury Plus 400 MHz NMR spectrometer at 25 °C. The polymer was dissolved with deuteronated chloroform and the ^1H spectrum was obtained with tetramethylsilane (TMS) as the internal reference.

2.2.3. Gel permeation chromatography (GPC)

The gel permeation chromatography (GPC) measurement was performed on a Perkin–Elmer Series-2000 GPC apparatus with DMF as solvent. The molecular weights were expressed relative to polystyrene standard.

2.2.4. Differential scanning calorimetry (DSC)

Thermal analysis was performed on a Perkin–Elmer Pyris-1 differential scanning calorimeter in dry nitrogen atmosphere. The instrument was calibrated with a standard Indium. In order to measure glass transition temperatures, all the samples (about 10.0 mg in weight for amorphous samples, 5.0 mg for crystalline samples) were first heated up to 150 °C and held for 5 min to remove thermal history, followed by quenching to −70 °C. A heating rate of 20 °C/min was used at all cases. Glass transition temperature (T_g) was taken as the midpoint of the heat capacity change. The crystallization temperatures (T_c) and the melting temperatures (T_m) were taken as the temperatures of the minima and the maxima of both endothermic and exothermic peaks, respectively.

In order to obtain the equilibrium melting point, all samples was heated up to 150 °C and hold for 5 min to removed thermal history, then quenching to desired crystallization temperature (T_c) for completion of crystallization, followed by the scans to 150 °C at the heating rate of 10 °C/min to measure the melting temperatures (T_m).

3. Results and discussion

3.1. Synthesis and characterization

The properties of PHEE are quite dependent on the type of diacids used. In this work, an aromatic diacid, terephthalate diacid was used instead of aliphatic acids used in the literature [1–15] to obtain the thermoplastic PHETE with the higher glass transition temperature. The polymerization between diglycidyl ether of bisphenol A (DGEBA) and terephthalate acid catalyzed with tetrabutylammonium bromide (TBAB) was exploited to prepare poly(hydroxyether terephthalate ester) (PHETE). Shown in Fig. 1 is the FTIR spectrum of PHETE. In the FTIR spectrum, the absorption bands at 3416 and 1722 cm^{-1} were ascribed to the stretching vibrations of hydroxyl and carbonyl groups, respectively, which were characteristic of the structural units of hydroxyether structural unit and terephthalate ester moiety. Fig. 2 shows the ^1H NMR spectrum of PHETE together with the assignment, respectively. From the results of FTIR and NMR, it is adjudged that the expected structure of PHETE was obtained by the reaction between DGEBA and terephthalate diacid in DMF solution. Gel permeation chromatography (GPC) experiment showed that this polymer possesses the high molecular weights of $M_n = 12{,}000$ and $M_w = 19{,}000$. The DSC result indicates that PHETE is an amorphous polymer with a glass transition temperature of $T_g = 88$ °C, which is close to that of PH ($T_g = 90$ °C). Due to the presence of both secondary hydroxyl and carbonyl groups in the macromolecular backbone PHETE could be a self-associated polymer and the self-association could be involved with two competitive intramolecular hydrogen

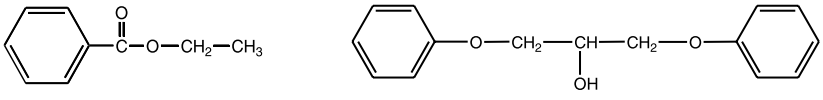

EB DPP

Scheme 2. Structures of ethyl benzoate (EB) and 1,3-diphenoxy-2-propanol (DPP).

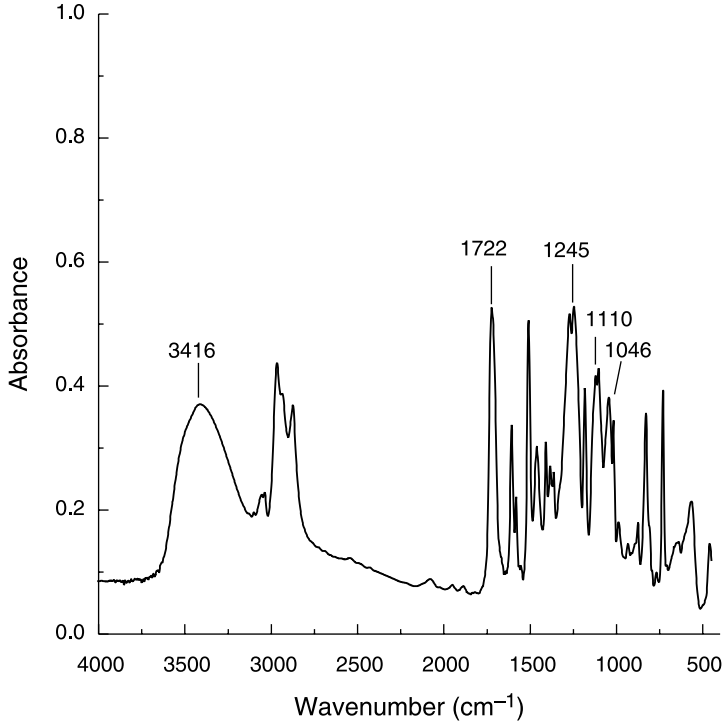

Fig. 1. FTIR Spectrum of poly(hydroxyether terephthalate ester).

bonding interactions, i.e. –OH···–OH and –OH···O=C< in the macromolecular chain of PHETE. Shown in Fig. 3 is the comparison of FTIR spectra for PHETE and PH in the hydroxyl stretching vibration range of 3100–3800 cm^{-1}. The broad bands reflect the wide distribution of hydrogen-bonded hydroxyl stretching frequencies. The shoulder bands centered at 3570 cm^{-1} are ascribed to the free hydroxyls [16]. It was noted that a new band at a higher frequency (~3504 cm^{-1}) is discernable, suggesting that there was the formation of the weaker hydrogen bonding interactions in PHETE than in PH. This observation could be ascribed to the formation of the weaker –OH···O=C< hydrogen bonding in stead of some –OH···–OH hydrogen bonding interactions.

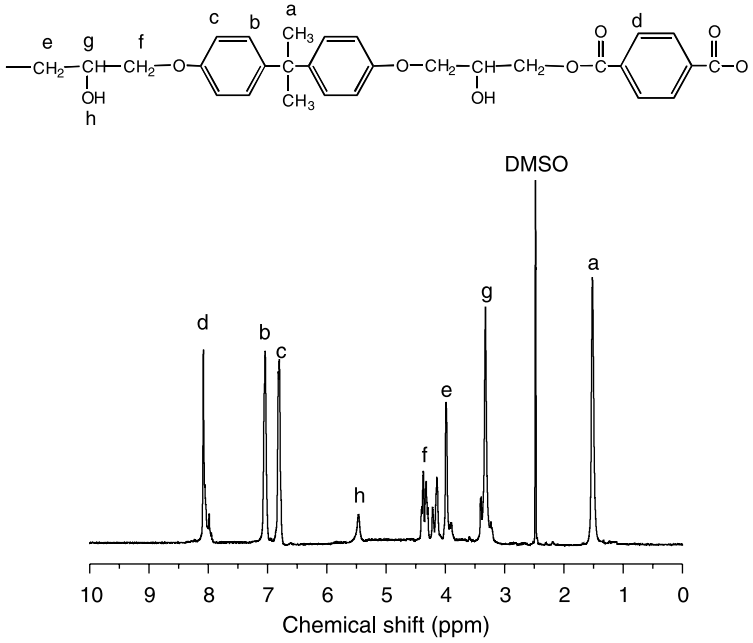

Fig. 2. ^{1}H NMR Spectrum of poly(hydroxyether terephthalate ester).

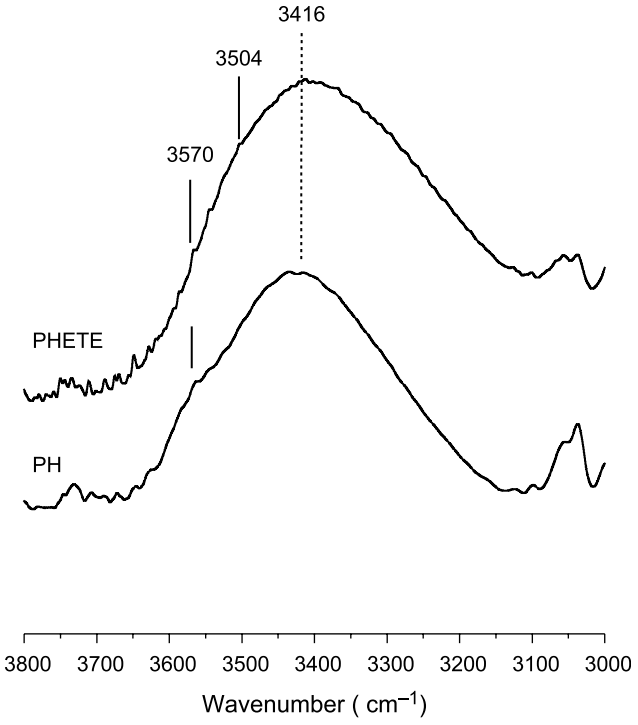

Fig. 3. Comparison of FTIR spectra in the region of 3000–3800 cm^{-1} for PHETE and PH.

3.2. Blends of PHETE and PEO

3.2.1. Miscibility

The PHETE/PEO blends were prepared via casting from THF solution and the homogenous and transparent films were obtained with the PEO content up to 40 wt%. The clarity of the blend films indicates that the PHETE/PEO blends present single amorphous phase, i.e. no phase separation occurred at least on a scale exceeding the wavelength of visible light. Nonetheless, the blend samples with PEO content exceeding 40 wt% are not transparent at room temperature. When heated up to 70 °C, i.e. above the melting point (~65 °C) of PEO, these samples became transparent, suggesting that the spherulites of PEO were formed in the PEO-rich blends.

The DSC curves of PHETE, PEO and their blends were presented in Fig. 4. It can be seen that each blend displayed a single glass transition temperature (T_g), intermediate between those of the two pure components and changing with the blend composition. In terms of the single and composition-dependent glass transition behavior, it is concluded that PHETE/PEO blends are miscible in the amorphous state, i.e. possess single homogeneous and amorphous phases. From Fig. 4, it is seen that for pure PEO, 10/90, 20/80 PHETE/PEO blends, no cold crystallization transitions were observed since crystallization was sufficiently rapid and occurred to completion during the quenching. However, the DSC curves of the blends containing 70, 60 and 50 wt% of PEO displayed cold crystallization phenomenon after glass transition and the

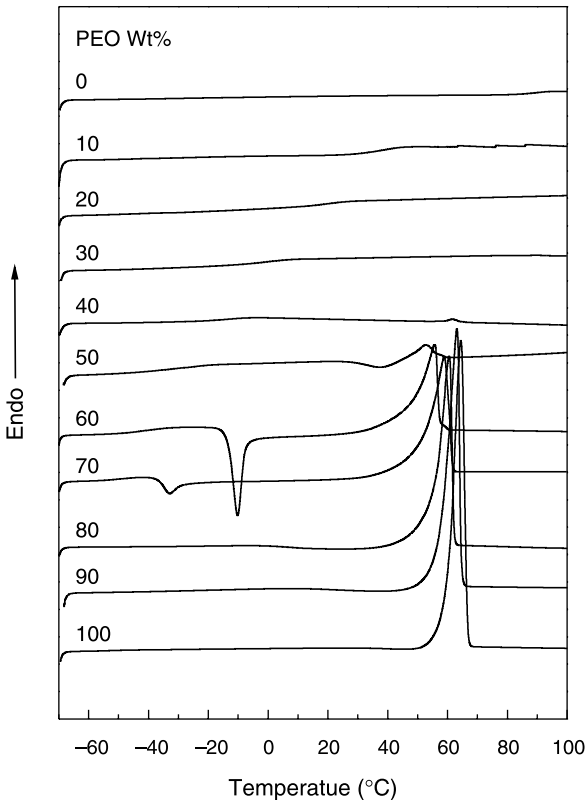

Fig. 4. DSC curves of PHETE/PEO blends.

crystallization temperatures (T_cs) increased with increase of PHETE content, indicating that the crystallization of PEO becomes progressively difficult in PHETE-rich blends. While PHETE content is more than 50 wt%, there is no melting transition of PEO in blends because the degree of supercooling (viz. $T_m - T_g$) is almost non-existent, i.e. the absence of significant supercooling restricts PEO from crystallization upon cooling from the molten state, which is required for crystallization to occur.

Fig. 5 shows the plot of crystallinity of PEO in the blends as a function of blend composition, which was calculated from the following equation:

$$X_c = \frac{(\Delta H_f - \Delta H_c)}{\Delta H_f^0} \times 100\% \quad (1)$$

where X_c is percent crystallinity. ΔH_f and ΔH_c are the enthalpy of fusion and crystallization of PEO, respectively. ΔH_f^0 is the fusion enthalpy of perfectly crystallized PEO, and has been reported to be 205 J/g [17]. The crystallinity of PEO in the blends containing PHETE dramatically deviates from the dashed line, which stands for the crystallinity of PEO in the blends if the crystallization process were not influenced by the presence of PHETE, suggesting a pronounced inhibition of crystallization by the presence of PHETE. The supercooling of PEO crystallization decreased with increasing PHETE contents in the miscible blends. The absence of significant supercooling will restrict PEO from crystallization upon cooling from the molten state; the

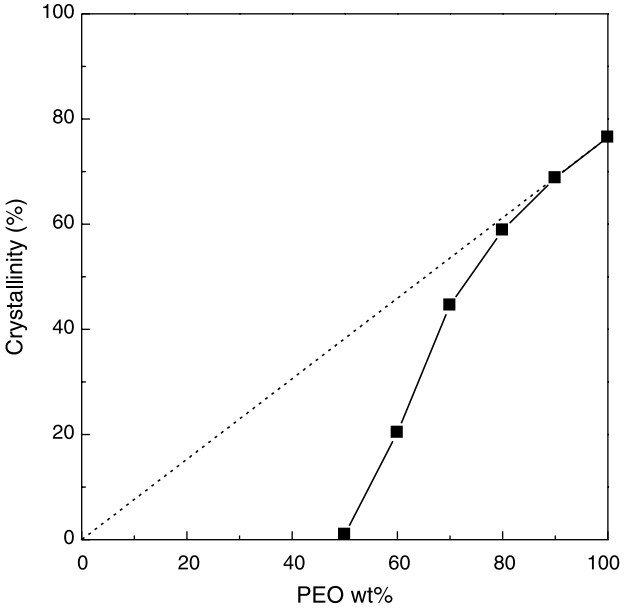

Fig. 5. Percent crystallinity of PEO in PHETE/PEO blends: (■) The second DSC traces; dashed line represents the crystallinity of PEO in blends if the crystallization process was not influenced by the presence of PHETE.

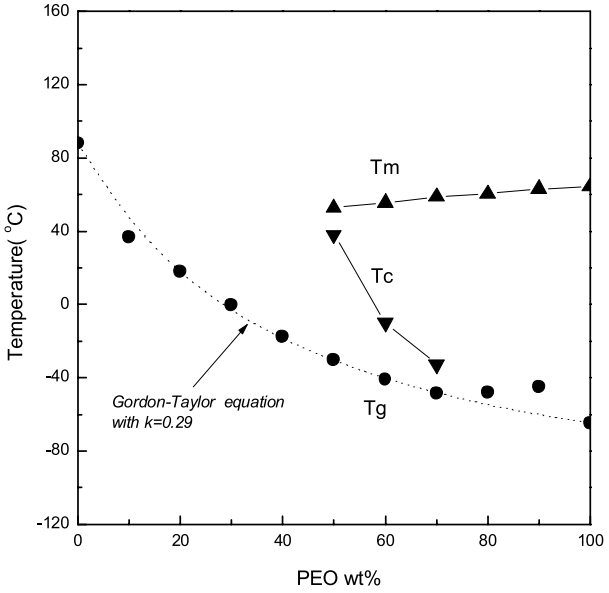

Fig. 6. Phase diagram of PHETE/PEO blends.

amorphous phase is vitrified and thus crystallinity decreases dramatically with increasing PHETE contents.

There are several theoretical and empirical equations to describe the dependence of glass transition temperature on blend composition [18–21]. Of them Gordon–Taylor [19] equation is mostly used:

$$T_g = \frac{W_1 T_{g1} + kW_2 T_{g2}}{W_1 + kW_2} \quad (2)$$

where W_i is the weight fraction of component i and T_g is the glass transition temperature of blend; k is the so-called Gordon–Taylor coefficient defined by:

$$k = \frac{v_2 \Delta\alpha_2}{v_1 \Delta\alpha_1} \quad (3)$$

where v_i is the specific volume of component i and $\Delta\alpha_i$ the difference between its volume expansion coefficient in the liquid and glassy state at T_{gi}. This equation can describe the effects of thermal expansion on the T_g. In general, the k is an adjusting parameter related to the degree of curvature of the T_g-composition curve. Prud'homme et al. [22,23] proposed that in miscible polymer blends, the quantity k can be taken as a semi-quantitative measure of strength of the intermolecular interaction between components of polymer blends. The application of Eq. (3) to the present experimental T_gs yielded a k value of 0.29, fitting the experimental T_gs quite well as shown in Fig. 6. It is interesting to note that the k value obtained for PHETE/PEO blends is quite lower than those (ca. 0.5) obtained for the blends of poly(hydroxyether of bisphenol A) (PH) with PEO [24–26], suggesting that the interchain specific interactions were significantly weakened with the inclusion of terephthalic diester moiety into PH macromolecular backbone. This observation could be ascribed to the decease in hydroxyl fraction in PHETE in comparison with PH. It should be pointed out that in the fitting the T_g values of PEO-rich blends (with PEO more than 70 wt%) were not used since there is the compositional enrichment of the amorphous region created by crystallization of PEO [27–29]. It was noted that the T_g of blends with PEO more than 70 wt% displayed the obvious positive deviation from the prediction by Gordon–Taylor equation. Returning to Fig. 4, it is seen that the melting temperatures (T_m) of PEO in the blends depressed, characteristic of miscible polymer blends. The crystallization temperatures (T_c) of PEO in the blends increased with increasing the content of PHETE, indicating the inhabitation effect of the amorphous component on crystallization in the miscible blends.

3.2.2. Equilibrium melting point depression

Analysis of equilibrium melting point for semi-crystalline polymer and amorphous polymer blends can give the information about miscibility and polymer–polymer interactions. Equilibrium thermodynamics predicts that by addition of a miscible diluent the chemical potential of the crystalline polymer will be decreased, which will result in the depression of equilibrium melting points. In the miscible polymer blends the melting points could be depressed due to thermodynamic and/or morphological reasons. To eliminate the morphological effect, the equilibrium melting points of PEO and its blends with PHETE were analyzed by Hoffman–Weeks method [30,31]. The plots of the experimental melting temperatures (T'_m) as a function of crystallization temperature (T_c) are shown in Fig. 7. It can be seen that in the range of the crystallization temperatures investigated, the T'_m increased linearly with the T_c. The

Table 1
Equilibrium melting points, the stability parameters and glass transition temperature, T_g for PHETE/PEO blends

PHETE/PEO (wt)	T_m^0 (°C)	Φ	T_g (°C)
0/100	69.0	0.158	−65.0
10/90	68.4	0.166	−44.8
20/80	67.5	0.180	−48.0
30/70	66.7	0.232	−47.7
40/60	65.5	0.267	−40.7

experimental data can be fitted by the Hoffman–Weeks equation [30,31]

$$T_m = \Phi T_c + (1-\Phi)T_m^0 \quad (4)$$

where T_m^0 is the equilibrium melting point; $\Phi = 1/\gamma$ is the stability parameter which depends on the crystal thickness, whereas γ is the ratio of the lamellar thickness l to the lamellar thickness of the critical nucleus l^* at T_c. In Eq. (4), Φ may assume the values between 0 and 1, $\Phi = 0$ implies $T_m = T_m^0$, whereas $\Phi = 1$ implies $T_m = T_c$. Consequently, the crystals are most stable for $\Phi = 0$ and inherently unstable for $\Phi = 1$. As shown in Fig. 7, the values of T_m^0 can be evaluated by extrapolating the least-squares fit lines of the experimental data according to Eq. (4) to the intersect the line of $T_m = T_m^0$. The Φ parameters can be determined from the slope of these fit lines. Both, the values of T_m^0 and of Φ for the blend composition investigated are summarized in Table 1. The values of the stability parameters Φ range from 0.158 to 0.267, suggesting that the crystals are quite stable. The data of equilibrium melting points obtained in the study were further analyzed with the Nishi–Wang equation [32,33], which is derived from the Flory–Huggins theory. The

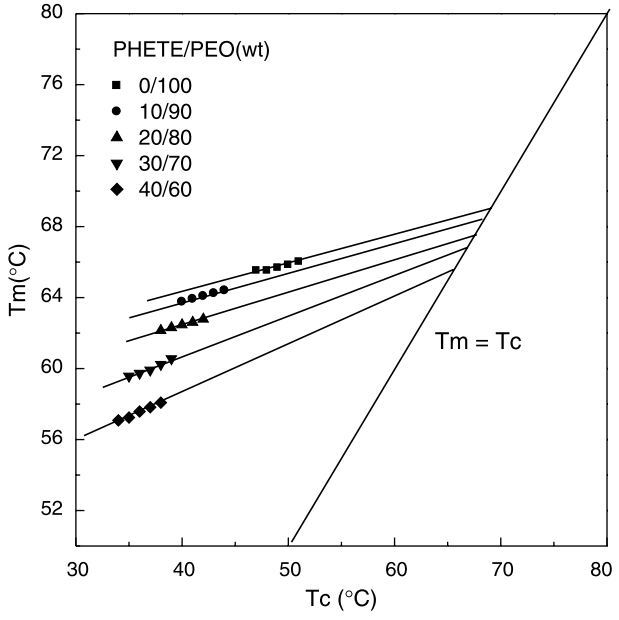

Fig. 7. Hoffman–Weeks plot for determination of equilibrium melting point (T_m^0) for PHETE/PEO blends.

Table 2
Data of FTIR difference spectra of mixture of toluene, DB and DPP at 25 °C for determination of K_C

C_{EB} (M)	C_{DPP} (M)	f_m^{OH}	K_C (L mol^{-1})
0	0.02	–	3.81[a]
0.02	0.02	0.939	3.46
0.06	0.02	0.863	2.77
0.10	0.02	0.843	1.62
0.15	0.02	0.825	1.45
0.20	0.02	0.800	1.28

[a] Extrapolated to $C_{EB} = 0$.

T_m depression is derived as follows:

$$\frac{1}{T_m^{0\prime}} - \frac{1}{T_m^0} = -\frac{BV_{2u}}{\Delta H_{2u}}\left(\frac{\phi_1^2}{T_m^{0\prime}}\right) \quad (5)$$

where the subscripts 1 and 2 denote the amorphous and crystalline components, respectively. ϕ_1 is the volume fraction, V_{2u} is the molar volume of the repeating unit, ΔH_{2u} refers to the fusion enthalpy per mole of 100% crystalline PEO. $T_m^{0\prime}$ and T_m^0 are the equilibrium melting points of the blends and the pure crystalline component. R is the universal gas constant. B is the interaction energy density. The interaction parameter χ_{12} can be written as:

$$\chi_{12} = \frac{BV_{1u}}{RT} \quad (6)$$

In this work, several constants were taken as $\Delta H_{2u} = 9020$ J/mol [17] and $V_{2u} = 38.9$ cm^3/mol. The value of $V_{1u} = 396.6$ cm^3/mol was estimated according to group contribution method [34]. Assuming that B (or χ) is composition-independent, a plot of the left terms of Eq. (6) versus ϕ_1^2/T_m^0 should yield a straight line with a slope

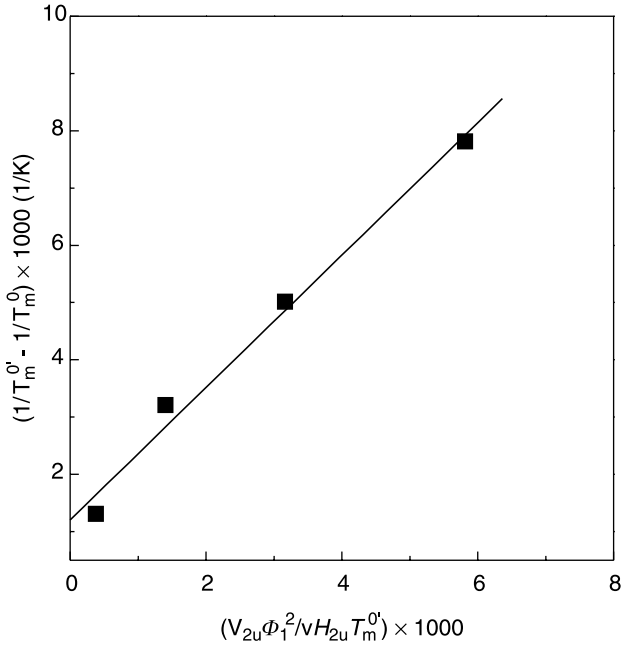

Fig. 8. Flory–Huggins equation plot for the equilibrium melting temperature obtained for PHETE/PEO blends.

proportional to B and zero y-intercept. From the slope, B and consequently χ_{12} were obtained to be -1.32 J/cm^3 and -0.18 at 344 K, and the negative value of B (or χ_{12}) suggests that the PHETE/PEO blends are miscible in the melt state (Fig. 8).

3.3. Specific interactions

3.3.1. Intramolecular hydrogen bonding interactions of PHETE

In view of the macromolecular structure, it is expected that PHETE is a self-associated polymer due to the presence of both secondary hydroxyl and carbonyl groups in the macromolecular backbone. The intramolecular specific interactions could be involved with –OH···–OH and –OH···O=C< hydrogen bonding. In order to describe intramolecular hydrogen bonding interactions of PHETE, three equilibrium constants are required. According to the Painter–Coleman association model [35,36], we used the subscripts 2, B and C to denote the equilibrium constants, K_2, K_B and K_C of dimers, multi-mers of PHETE and the association of PHETE via –OH···O=C< hydrogen bonding, respectively:

$$B + B \overset{K_2}{\leftrightarrow} B_2 \tag{7}$$

$$B_h + B \overset{K_B}{\leftrightarrow} B_{h+1} \tag{8}$$

$$B_h + C \overset{K_C}{\leftrightarrow} B_hC \tag{9}$$

Both Eqs. (7) and (8) represent the self-association of hydroxyl ether structural units in PHETE via –OH···–OH hydrogen bonding whereas Eq. (9) stands for the intra-chain association of –OH···O=C< in PHETE. The values of K_2 and K_B have been measured to be $K_2=12.9$ (dimensionless unit), $K_B=21.3$ (dimensionless unit) and $K_2=14.4$ (dimensionless unit), $K_B=25.6$ (dimensionless unit) by Coleman et al. [35] and Iruin et al. [37], respectively. In the present work, we need to obtain the additional equilibrium constant, K_C to account for the intramolecular hydrogen bonding interaction between the hydroxyl and carbonyl groups. To this end we chose 1,3-diphenoxy-2-propanol (DPP) and ethyl benzoate (EB) as the model compounds of the hydroxyether structural unit and carbonyl moiety in PHETE (Scheme 2) and investigate the intramolecular hydrogen bonding interactions by following the evolution of the infrared bands of the hydroxyl group in the toluene solutions of the mixture of DPP with EB as functions of concentrations to measure K_C. By increasing the concentration of EB from 0.02 to 0.2 M and keeping the constant of DPP concentrate (0.02 M), the fraction of free monomers was measured. For simple alcohols and phenols it is assumed that the intensity of free hydroxyl band is a measure of free monomers [35,36,38]. The intensity (absorbance) of the isolated hydroxyl band, I, is related to the absorptivity coefficient, ε, the concentration, c, and the path length l, by Beer-Lambert law, $I=\varepsilon lc$. The experimental fraction of the free monomer, f_m^{OH} at any given concentration of DPP was calculated by Eq. (10).

$$f_m^{OH} = \frac{I}{I_0} \tag{10}$$

where I_0 is the absorbance of the hydroxyls of the pure DPP. As shown in Fig. 9 are the FTIR difference spectra in the hydroxyl stretching region for the mixture of EB, DPP and toluene. It is seen that the intensity (fraction) of the free hydroxyl (at 3580 cm^{-1}) of DPP decreased with increasing EB concentration while intensity of the hydrogen-bonded hydroxyl bands (i.e. dimer) at lower frequency, indicating that more fraction of hydrogen bonding was formed. The results were summarized in Table 2. To calculate K_C based on the FTIR results, following equation is used [35,36,38]:

$$K_C = \frac{1 - f_m^{OH}}{f_m^{OH}\left(C_C - \left(1 - f_m^{OH}\right)C_B\right)} \tag{11}$$

where C_C and C_B denote concentration of EB and DPP in L mol^{-1}, respectively. According to Eq. (11), $K_C=3.81$ is obtained. The K_C value is quite lower than the values of K_2 ($=12.9$) and K_B ($=21.3$), suggesting that the hydrogen bonding interactions between hydroxyl and carbonyl groups are significantly weaker than the strength of hydroxyl versus hydroxyl groups. This result is in a good agreement with the comparison between hydroxyl stretching vibration bands of PH and PHETE, as shown in Fig. 3.

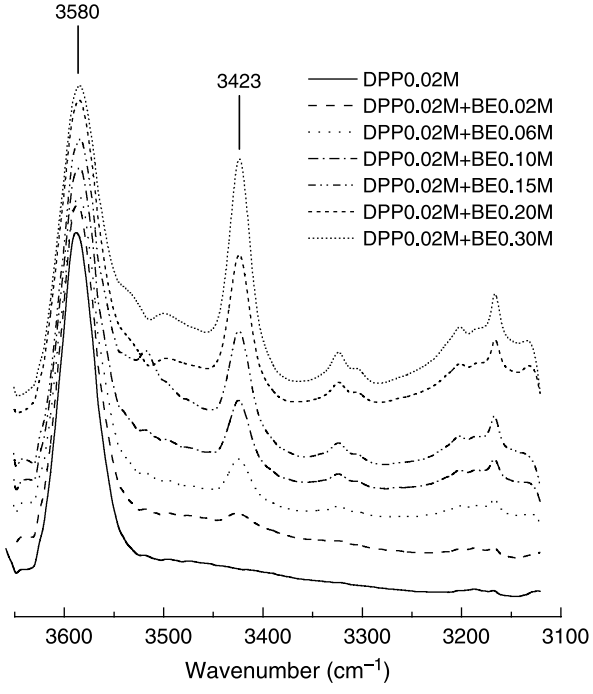

Fig. 9. FTIR difference spectra of EB/DPP/toluene solutions with various EB concentrations for determination of K_C.

3.3.2. Competitive hydrogen-bonding interactions

Upon adding PEO to the system, the new equilibriums of hydrogen bonding association will be established among –OH···O=C<, –OH···–OH and hydroxyl versus ether oxygen atom of PEO, which could be involved with the break of the self-associated hydrogen bonds of PHETE and the formation of the intermolecular hydrogen bonds between PHETE and PEO to some extent. Since there are differences in the strength of above hydrogen bonding interactions, it is expected that there could be the competitive specific interactions in the miscible blends [39]. Shown in Fig. 10 are FTIR spectra of pure PHETE and its blends with PEO in the region of 3000–3800 cm^{-1}. In this frequency region, the spectroscopic bands are ascribed to hydroxyl stretching vibration. For pure PHETE, the stretching vibration bands of the associated hydroxyl groups comprised of two components at 3504 and 3416 cm^{-1}, respectively. The former is ascribed to the hydroxyl groups H-bonded with carbonyl groups whereas the latter to the self-associated hydroxyl groups (viz. –OH···–OH). It should be pointed out that the stretching vibration of free hydroxyl groups occurs at 3570 cm^{-1} [16] although this band is quite weak for PHETE. Upon adding PEO to the system, it was noted that the hydroxyl stretching vibration shifted to the lower frequencies (i.e. 3316 cm^{-1}). The band at 3316 cm^{-1} could be ascribed to the hydroxyl groups that were H-bonded with the ether oxygen atoms of PEO. In the meantime, the intensity of the bands at 3504 and 3416 cm^{-1} decreased and the intensity of the band at 3316 cm^{-1} increased with increasing the content of PEO. The low-frequency shift of the stretching vibration of hydroxyl groups indicates that the intermolecular hydrogen bonding interactions between PHETE and PEO are much stronger than those of the self-association of PHETE via –OH···–OH and –OH···O=C< hydrogen bonds. The frequency difference ($\Delta\nu$) between the free and H-bonded hydroxyl stretching vibration is a measure of the average strength of the intermolecular and/or intramolecular interactions [40,41]. For PHETE, we attributed the value of $\Delta\nu = 66$ cm^{-1} to the hydroxyls which were H-bonded with carbonyl groups (i.e. at 3504 cm^{-1}) whereas the value of $\Delta\nu = 154$ cm^{-1} to the hydroxyl groups via –OH···–OH association. The shift of both bands to lower frequencies indicated that the hydrogen bonding interactions between hydroxyls of PHETE and ether oxygen atoms of PEO are much stronger than those of –OH···–OH and –OH···O=C< hydrogen bonds. In terms of the frequency differences between free and H-bonded hydroxyl stretching vibration, it is judged that from weak to strong the strength of the hydrogen bonding interactions is in the following order: –OH···O=C<, –OH···–OH and –OH versus ether oxygen atoms of PEO.

The above results can be further confirmed with the variation of the association degree of PHETE carbonyls as a function of PEO weight fraction. Shown in Fig. 11 are the FTIR spectra of the blends in 1640–1840 cm^{-1}. For the pure PHETE, it is seen that the infrared band is quite broad and asymmetrical. There appeared shoulder bands at the

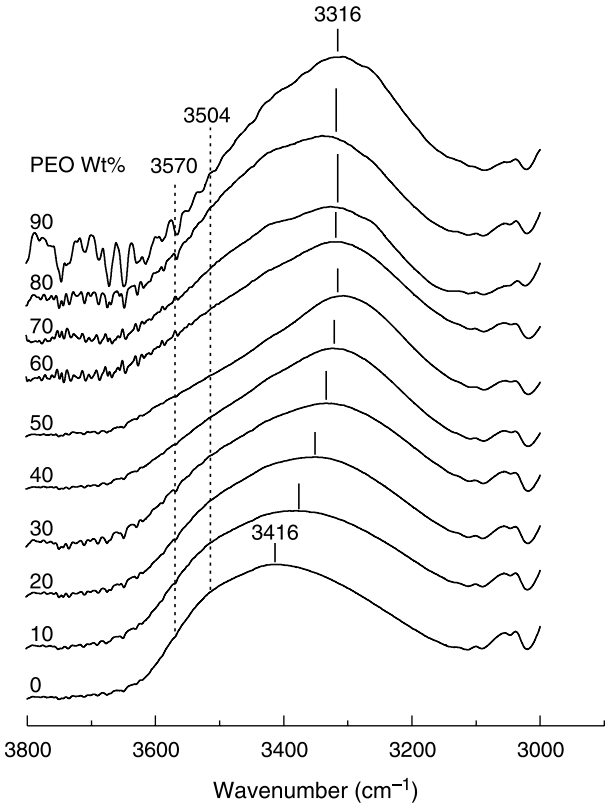

Fig. 10. FTIR Spectra of PHETE/PEO blends in the region of 3000–3800 cm^{-1}.

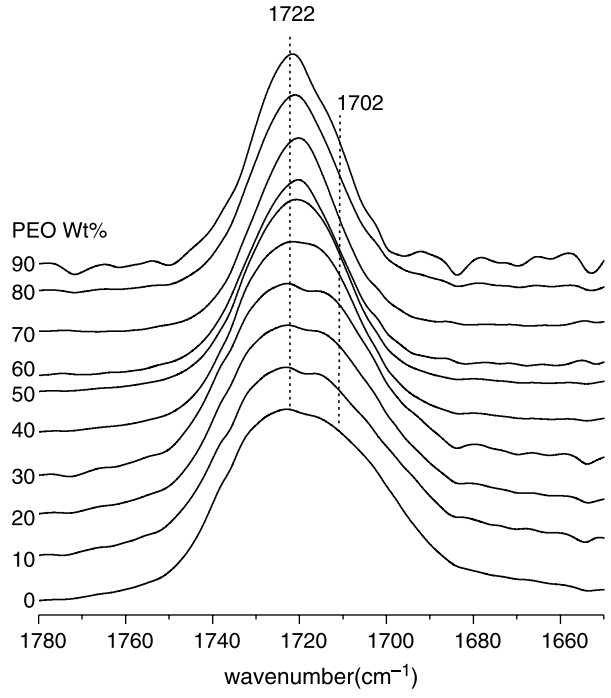

Fig. 11. FTIR Spectra of PHETE/PEO blends in the region of 1650–1850 cm^{-1}.

lower frequencies at 1702 cm^{-1}. The shoulder band could be ascribed to the stretching vibration of hydrogen-bonded carbonyls. Upon adding PEO to the system, it is interesting to note that the intensity of the shoulder band is significantly reduced. When the content of PEO is 90 wt%, the stretching band of the carbonyl groups has been quite symmetrical, i.e. the portion of associated carbonyl groups is quite small and that the carbonyls of PHETE mainly exist in the blends in the non-associated form. The Gaussian line-shape function was used in this fitting procedure and the good fitting was carried out for the blends. The F_{co}^{f} is the fraction of the non-associated carbonyl bands, calculated from the values of absorbency for the associated and the non-associated band contributions:

$$F_{co}^{f} = \frac{A_f}{A_f + \left(\frac{\varepsilon_f}{\varepsilon_a}\right)A_a} \tag{12}$$

where ε_i is the molar absorption coefficient. The subscripts, f and a stand for free and associated carbonyl groups, respectively. To carry out this calculation, we require the knowledge of the molar absorption coefficients (ε_f and ε_a) or their ratio ($\varepsilon_f/\varepsilon_a$) for the non-associated and associated carbonyl bands. Using the $\varepsilon_f/\varepsilon_a$ value of 1.3 for the inter-association of ester type carbonyls determined by Coleman et al. [37,42], we calculated the fraction of non-associated carbonyl bands. The variation of F_{co}^{f} as a function of temperature is shown in Fig. 12. The curve-fitting results show that the molar fractions of free carbonyls are 90% for PHETE/PEO 90/10 mixture, i.e. the initial carbonyl groups associated with hydroxyl groups were increasingly released with PEO being added to the system.

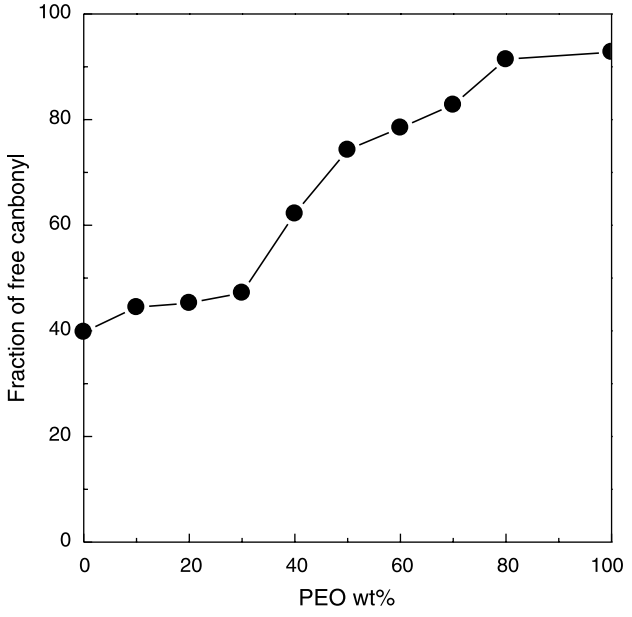

Fig. 12. Plot of fraction (F_{co}^{f}) of free carbonyl as a function of composition for the blends of PHETE and PEO.

4. Conclusions

Poly(hydroxyether terephthalate ester) (PHETE) was synthesized via the polymerization of diglycidyl ether of bisphenol A with terephthalic acid catalyzed by tetrabutylammonium bromide (TBAB). The miscibility and intermolecular specific interactions in the blends of PHETE with poly(ethylene oxide) (PEO) was investigated by means of differential scanning calorimetry (DSC) and Fourier transform infrared spectroscopy (FTIR). The PHETE/PEO blends displayed single and composition-dependent glass transition temperatures (T_gs), indicating that the blends are miscible in amorphous state, which was further confirmed by the depression of equilibrium melting point depression. FTIR studies indicate that there are the competitive hydrogen bonding interactions upon adding PEO to the system, which was involved with the intramolecular and intermolecular hydrogen bonding interactions, i.e. –OH···O=C<, –OH···–OH and –OH versus ether oxygen atoms of PEO between PHETE and PEO. In terms of the infrared spectroscopic investigation of the model compound and PHETE/PEO blends, it is judged that from weak to strong the strength of the hydrogen bonding interactions is in the following order: –OH···O=C<, –OH···–OH and –OH versus ether oxygen atoms of PEO.

Acknowledgements

The financial support from Ministry of Education, PRC under an Excellent Young Teacher Program (EYTP, No. 2066) was acknowledged. The authors would like to thank Natural Science Foundation of China (No. 20474038 and 50390090) and Shanghai Education Development Foundation, China under an Award (2004-SG-18) to 'Shuguang Scholar'.

References

[1] Mang MN, White JE. US Patent, 1,171,820; 1992.
[2] Mang MN, White JE, Swanson PE. US Patent, 5,496,910; 1996.
[3] Mang MN, White JE, Haag AP, Kram SL, Brown CN. Polym Prepr 1995;36:180.
[4] Rick DL, Davis JW, Kram SL, Mang MN, Lickly TD. J Environ Polym Degrad 1998;6:143.
[5] Mang MN, White JE, Kram SL, Rick DL, Bailey RE, Swanson PE. Polym Mater Sci Eng 1997;76:412.
[6] Shogren RL, Noane WM, Garlotta D, Lawton JW, Willet JL. Polym Degrad Stab 2003;79:405.
[7] Willet JL, Doane WM. Polymer 2002;43:4413.
[8] Walia PS, Lawton JW, Shogren RL, Felcker FC. Polymer 2000;41:8083.
[9] Lawrence SS, Willet JL, Carriere CJ. Polymer 2001;42:5643.
[10] Zhou G, Willett JL, Carriere CJ, Wu YV. J Polym Environ 2000;8:145.
[11] Wang C, Carriere CJ, Willett JL. J Polym Sci, Part B: Polym Phys 2002;40:2324.

[12] Cao X, Mohamed A, Gordon SH, Willet JL, Sessa DJ. Polym Prepr 2001;42:652.
[13] Willet JL, Doane W. US Patent, 6,191,196; 2001.
[14] Cao X, Mohamed A, Gordon SH, Willet JL, Sessa DJ. Polym Prepr 2001;42:623.
[15] Cao X, Mohamed A, Gordon SH, Willet JL, Sessa DJ. Thermochim Acta 2003;406:115.
[16] Coleman MM, Moskala EJ. Polymer 1983;24:251.
[17] Vidotte G, Levy DL, Kovacs AJ. Kolloid ZZ Polym 1969;230:289.
[18] Fox TG. Bull Am Phys Soc 1956;1:123.
[19] Gordon M, Taylor JS. J Appl Chem 1952;2:496.
[20] Couchman PR. Macromolecules 1978;11:1156.
[21] Woo EW, Chiang C-P. Polymer 2004;45:8415.
[22] Belorgey G, Prud'homme RE. J Polym Sci, Part B: Polym Phys 1982; 20:191.
[23] Belorgey G, Aubin M, Prud'homme RE. Polymer 1982;23:1051.
[24] Li X, Hsu XL. J Polym Sci, Part B: Polym Phys 1984;22:1331.
[25] Itiarte M, Irerren JI, Etxeberria A, Iruin JJ. Polymer 1989;30:1160.
[26] Zheng S, Jungnickel B-J. J Polym Sci, Part B: Polym Phys 2000;38: 1250.
[27] Li Y, Stein M, Jungnickel B-J. Colloid Polym Sci 1991;269:772.
[28] Li Y, Jungnickel B-J. Polymer 1993;34:9.
[29] Jungnickel B-J. Curr Trends Polym Sci 1997;2:157.
[30] Hoffman JD, Weeks JJ. Res Natl Bur Stand 1962;66:13.
[31] Hoffman JD, Weeks JJ. J Chem Phys 1962;37:13.
[32] Nishi T, Wang TT. Macromolecules 1975;8:809.
[33] Imken RL, Paul DR, Barlow JW. Polym Eng Sci 1976;16:593.
[34] Van Krevelen DW. Properties of polymers: Their estimation and correlation with chemical structure. Amsterdam: Elsevier Scientific Publishing; 1976.
[35] Coleman MM, Painter PC. Prog Polym Sci 1995;20:1.
[36] Coleman MM, Graf JF, Painter PC. Specific interactions and the miscibility of polymer blends. Lancaster, PA: Technomic Publishing; 1991.
[37] Espi E, Alberdi M, Fernandez-Berridi MJ, Iruin JJ. Polymer 1994;35: 3712.
[38] Coggesshall DD, Saier EL. J Am Chem Soc 1951;73:5414.
[39] Lu H, Zheng S, Tian G. Polymer 2004;45:2897.
[40] Purcell KF, Drago RS. J Am Chem Soc 1968;24:251.
[41] Coleman MM, Painter PC. Appl Spectrosc Rev 1984;20:225.
[42] Hu Y, Motze HR, Etxeberria AM, Fernandez-Berridi HJ, Iruin JJ, Painter PC, et al. Macromol Chem Phys 2000;201:705.